Simulation of Corrosion Induced Damage of Reinforced Concrete

S. F. U. Ahmed* and M. Larner**

**Department of Civil Engineering, Curtin University, Perth, Australia.*

***AECOM Pty. Ltd., Perth, Australia.*

ABSTRACT

This paper presents a finite element (FE) based numerical model to simulate the corrosion-induced cracking of reinforced concrete. Both uniform and non-uniform corrosion of steel in concrete is simulated. The effect of non-uniform corrosion distribution, cover depths, cover-to-rebar diameter ratio and compressive strengths of concrete on the cracking and cracking pressure are studied. The results indicate that the pressure required to cause the cracking of concrete cover under non-uniform corrosion are much smaller, between 40% and 50%, than those under uniform corrosion. The model predicts that the pressure require to cause the cracking of the concrete cover increases as the concrete compressive strength increases. It is also found that as the cover to rebar diameter ratio is increased, the pressure require to cause the cracking of concrete cover increases with a linear relationship between cover depth-to-rebar diameter ratio and pressure required to cause cracking of the concrete cover. The model is also verified with the experimental results.

KEYWORDS: Corrosion, numerical model, reinforced concrete.

INTRODUCTION

Corrosion of steel reinforcement is recognized as the principal cause of deterioration of concrete structures (Williamson and Clark, 2000). Repairing costs due to concrete cracking and spalling of corroded reinforced concrete (RC) structures exceed those from other forms of deterioration by a substantial margin (Li et al., 2005). The cause of damage is mainly due to the expansion of corrosion products, which normally occupy a much larger volume than the volume of steel removed. The magnitude of this volume increase varies between 2 and 6 times the volume of metal removed. As corrosion progresses, the corrosion product grows in size and applies increasing mechanical forces to the surrounding concrete. This causes the concrete to crack and with further corrosion these cracks propagate, followed by spalling and delamination of concrete cover. This leads to a number of undesirable consequences such as a loss of load carrying capacity, loss of serviceability, reduction in structural safety, or simply an unpleasant appearance. Therefore, it is necessary to realistically determine the critical corrosion amount that causes the initiation of cracking in concrete cover.

Different methods have been used to study the response of corroded reinforced concrete. Experimental based testing is extremely time consuming and the use of materials can be quite costly (Mackerle, 1999). Moreover, existing structures cannot be tested at ultimate failure. This situation has strongly encouraged the development of advanced analytical models capable of representing corrosion induced cracking in RC structures under all possible loading conditions. The use of finite element analysis to study these components has been used in recent years. A definitive technique for analyzing reinforced concrete, one of the most used composite materials in construction, has been difficult to develop (Biggs et al., 2000). Finite element analysis methods work extremely well for materials such as steel and aluminum, which have well-defined material properties. The complex behavior of concrete is less predictable, which is a major factor that limits the capabilities of the finite element method.

In this study, a finite element based numerical model is developed to simulate the corrosion-induced cracking of reinforced concrete beams made with ordinary concrete. The critical corrosion amount that causes surface cracking of concrete cover is determined and explored. The effects of cover to rebar diameter (c/d) ratio, concrete strength, and corrosion pressure distribution due to the expansion of corrosion products on cracking pressure are investigated. The commercially available finite element program Strand7 (2011) is used in this study.

ANALYSIS

Material Model for Concrete

In this study, concrete is assumed to be a homogeneous and isotropic material. The stress-strain curve for concrete in uniaxial compression used in this analysis is shown in Figure 1 (a), where f'c is concrete compressive strength at 28 days in MPa, ε_0 is concrete strain at ultimate strength and ε_u is concrete strain at crushing strength. The parabolic shape of the compressive stress-strain curve's ascending branch is estimated using the following equation (Park and Paulay, 1975):

$$\sigma c = f'c \left[\frac{2\varepsilon c}{\varepsilon 0} - \left(\frac{\varepsilon c}{\varepsilon 0}\right)^2\right] \text{ for } \varepsilon_c \leq \varepsilon_0 \qquad [1]$$

where f'c is the concrete compressive strength at 28 days and ε_0 is defined as

$$\varepsilon_0 = \frac{2f'c}{Ec} \qquad [2]$$

where Ec is the Young's modulus of concrete.

The behavior of concrete in tension is modeled linear elastic up to the ultimate tensile strength. The stress-strain relationship is assumed linear with the initial elastic modulus of concrete up to ultimate tensile strength f'_{ct}. As shown in Figure 1 (b), beyond the point ε_u, the stress is reduced to zero. It is assumed that there is no strain softening.

Warner et al. (1998) suggest that an estimate of the characteristic principal tensile strength at 28 days is given as

$$f'_{ct} = 0.4 \sqrt{f'_c} \qquad [3]$$

where both strengths are in MPa.

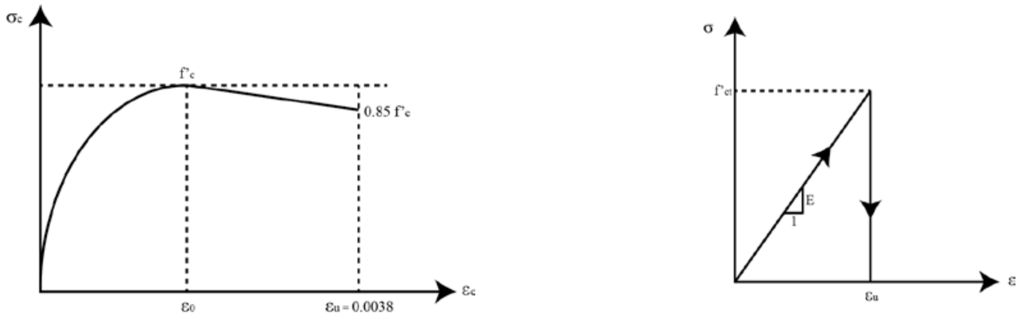

(a) Uniaxial Compression (b) Uniaxial Tension

Figure 1: Idealised stress-strain curves for concrete.

Yield Criterion

Concrete deforms in a non-linear, inelastic manner. A linear elastic assumption is not acceptable because the size and shape of the plastic zone may change as the applied load is increased and also as the crack length increases. In this study, an elastic-plastic material model is used for concrete plate elements.

The Mohr-Coulomb yield criterion used to model concrete in this study is described as follows:

$$\tau = c - \sigma \tan \phi \qquad [4]$$

where τ is shear stress on any plane, σ is normal stresses on any plane, c is cohesion and ϕ is the angle of internal friction.

The angle of internal friction (ϕ) is assumed to be 37° (Arslan, 2007) and the cohesion (c) is calculated as follows (Arslan, 2007) :

$$c = 0.75\, f'c^{\,0.31} \qquad [5]$$

where f'c is concrete compressive strength at 28 days and c is cohesion.

FINITE ELEMENT MODEL

Model Geometry

Even though the real problem is three-dimensional, a two-dimensional representation is deemed adequate. Creating a two-dimensional model will give similar results with much greater computational efficiency. Rectangular concrete beams with a cross-section of 160 x 160 mm are modeled. A void is created in the model to represent a reinforcement bar. A plate edge pressure is then applied to the elements surrounding the void. For the concrete beam model, as shown in Figure 2 (c), the bottom left node was fixed in translation and rotation about all axes. The bottom right node was fixed in y-axis translation and rotation about the z-axis. All other nodes are free to rotate and translate.

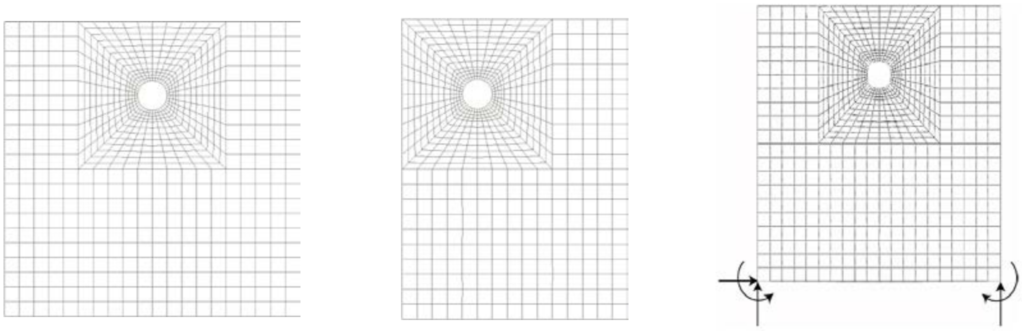

(a) Centre bar location (b) Corner bar location (c) Nodal restraint in beam model

Figure 2: Finite element meshes.

Corrosion Pressure Distribution

In order to explore the effects of corrosion distribution types (α), the values considered in this study range from 1 to 8. Gonzalez et al. (1995) have reported that the value of α ranges from 4 to 8 in natural conditions. Corrosion distributions were converted to a pressure (MPa), which is applied to the element edge in the model (see Figure 3).

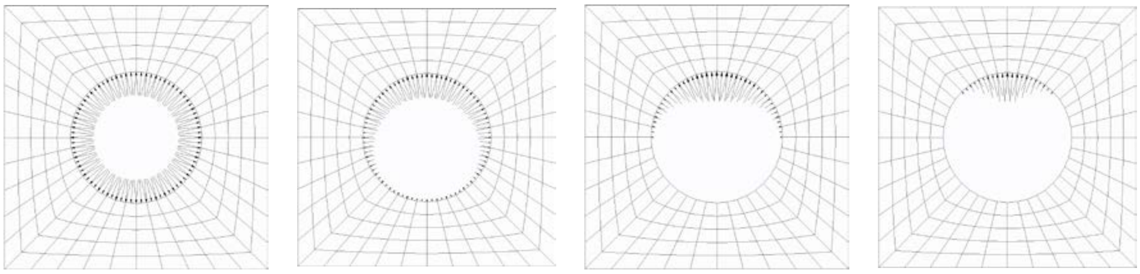

(a) uniform pressure $\alpha = 1$ (b) non-uniform pressure $\alpha = 2$ (c) non-uniform pressure $\alpha = 4$ (d) non-uniform pressure $\alpha = 8$

Figure 3: Uniform and non-uniform pressure distributions around reinforcement bar (Jang and Oh, 2010)**.**

Analysis Procedure

The incremental method of applying load with a non-linear load stepping is adopted in the application of cracking pressure in this model. The cracking pressure increases until the model showed failure. Failure in the model occurred when the stress in the elements reached the ultimate tensile strength of concrete. At this stage, cracks are assumed to form and propagate. The cracking pressure is defined as the expansion pressure at which cracking occurs at the concrete surface. As displacements are quite small, geometric nonlinearities are neglected. The model uses the implicit Newton-Raphson procedure to account for material non-linearity in this study.

CONVERGENCE ANALYSIS

In finite element analysis a finer mesh typically results accurate solution for stress analysis. However, as the mesh is made finer the computation time increases. A mesh convergence analysis is conducted to obtain the optimum mesh density as shown in Figure 4. The figure shows that, for a typical FE model with centre bar location (see Figure 2a), the cracking pressure decreases as the number of elements increases in the model up to number of elements 180. Any further increase in element number doesn't significantly decrease the cracking pressure indicating the optimum mesh density of the model.

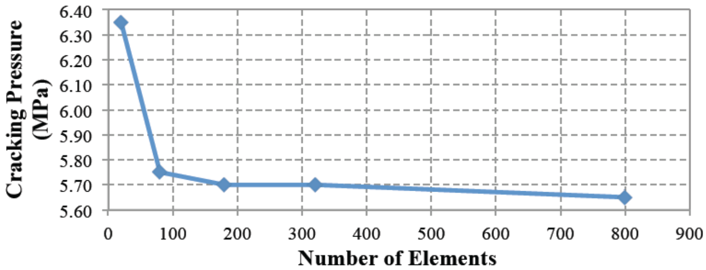

Figure 4 Effect of number of elements on the cracking pressure

RESULTS AND DISCUSSION

Effect of corrosion distribution on the cracking pressure

The effect of corrosion distribution on the cover cracking of RC is shown in Figure 5. It can be seen that uniform corrosion ($\alpha = 1$) and mild non-uniform corrosion ($\alpha = 2$) exhibited very similar cracking pressure. This isn't the case for a more localized pitting corrosion such as medium and severe non-uniform corrosions ($\alpha = 4$ and $\alpha = 8$) which show a 45% and 60% decrease in cracking pressure, respectively. These results suggest that a localized pitting corrosion can cause the concrete cover to crack at low expansion pressures, which is often the case in real conditions (Gonzalez et al., 1995). Figure 6 shows the effect of degree of pitting corrosion on the cracking pressure of concrete cover. It shows that the pressure required to causes the cover cracking decreases with increase in the degree of pitting corrosion (i.e. the alpha values) irrespective of cover depth.

Effect of Concrete Compressive Strength on the cracking pressure

The effect of concrete compressive strength on the cracking pressure and stress distribution around a reinforcing bar is shown in Figure 7. It can be seen that although the stress distribution looks identical, the pressure required causing cracking of the concrete cover increases as the concrete compressive strength increases.

Figure 8 shows cracking pressure as a function of concrete compressive strength for various types of corrosion distribution (α). It indicates that with increase in the degree of pitting corrosion (α value is increased) the pressure required to cause cracking of the concrete cover is decreased.

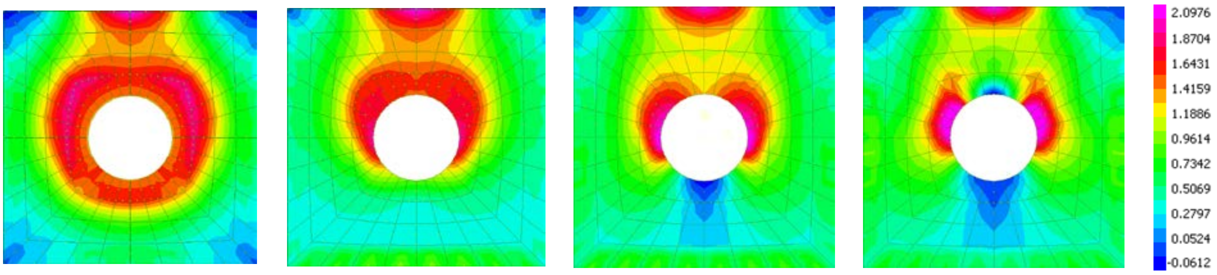

P_{cr} = 3.20 MPa (a) uniform corrosion $\alpha = 1$

P_{cr} = 3.10 MPa (b) non-uniform corrosion $\alpha = 2$

P_{cr} = 1.75 MPa (c) non-uniform corrosion $\alpha = 4$

P_{cr} = 1.30 MPa (d) non-uniform corrosion $\alpha = 8$

Figure 5: Effect of non-uniform corrosion on the cracking pressure (P_{cr}).

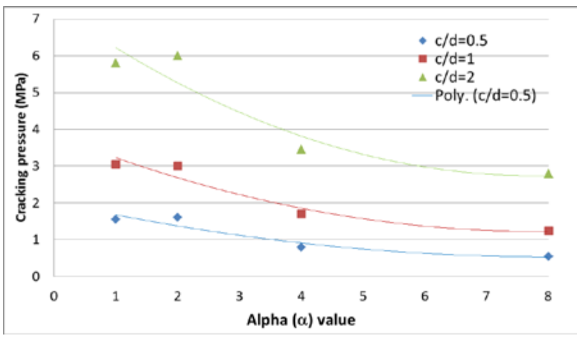

Figure 6: Effects of corrosion distribution and concrete cover on the cracking pressure.

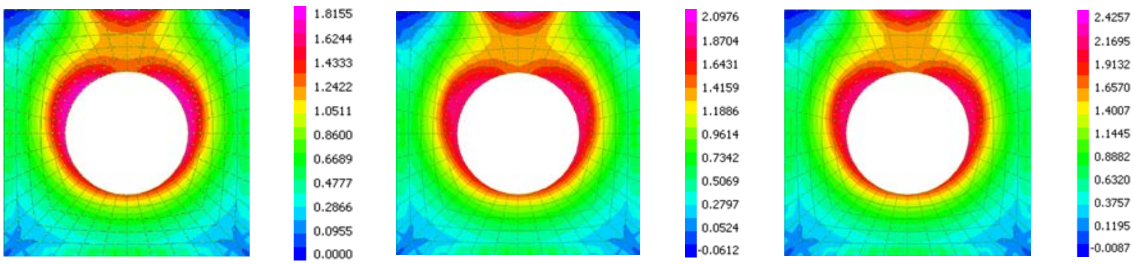

P_{cr} = 1.35 MPa (a) f'_c = 20.6 MPa

P_{cr} = 1.55 MPa (b) f'_c = 27.5 MPa

P_{cr} = 1.80 MPa (c) f'_c = 44.1 MPa

Figure 7: Effect of concrete strength on the cracking pressure P_{cr}

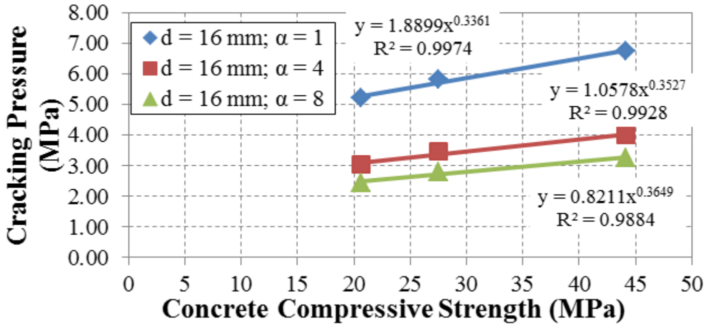

Figure 8: Cracking pressure as a function of compressive strength for various α values

Effect of concrete cover and bar diameter on the cracking pressure

The effect of cover depth on the cracking pressure in concrete is shown below in Figure 8.

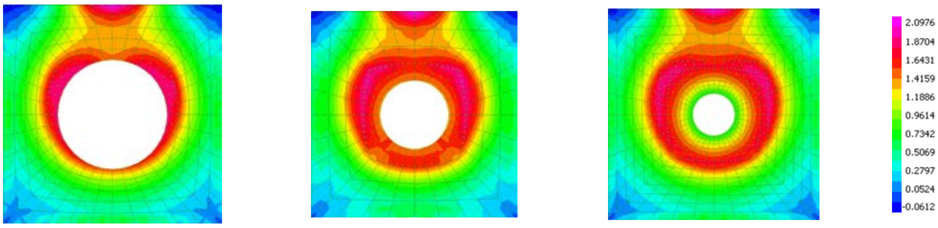

P_{cr} = 1.55 MPa (a) c/d = 0.5 | P_{cr} = 3.20 MPa (b) c/d = 1.0 | P_{cr} = 5.85 MPa (c) c/d = 2.0

Figure 9: Effect of cover depth on the cracking pressure (P_{cr})

Figures 8 and 9 suggest that as the cover depth is increased, the corrosion pressure required to cause the cracking of the concrete cover increases. It can be seen in Figure 10 that the relationship between cover depth-to-rebar diameter ratio and pressure required to cause cracking of the concrete cover is linear irrespective of bar diameter and corrosion types.

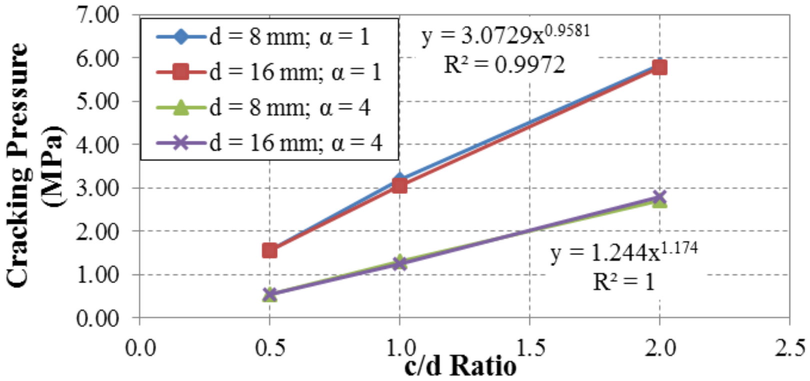

Figure 10: Effect of bar diameter, cover depth-to-bar diameter ratio on the cracking pressure of uniform and pitting corrosion

VERIFICATION OF MODEL

The model is also verified with the existing experimental results on corrosion induced cracking of concrete. Figure 11 shows the comparison of model predicted cracking pressure with that obtained in the experiment by Williamson and Clark (2000). In the study by Williamson and Clark (2000), hydraulic pressurisation of hollow concrete specimens was used to simulate the expansive pressure created by uniform corrosion. Uniform corrosion was modelled using a hydraulic jack to pressurise a soft PVC tube inserted into the hollow concrete specimens. The specimens were incrementally loaded to failure using a hand pump with a mounted pressure gauge. Tests were carried out in order to investigate the magnitude of pressure created by corrosion products on steel in reinforced concrete that would cause surface cracking of the concrete cover. It can be seen in Figure 10 that a good correlation between analytical and experimental results are obtained indicating the validity of the present model.

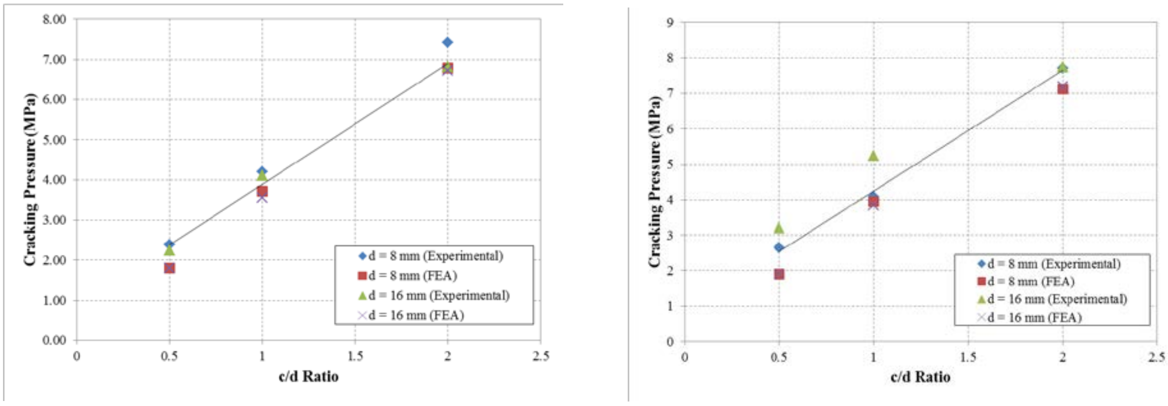

Figure 11: Comparison of model result with experimental data (Williamson and Clark, 2000) (Left figure: rebar at the centre and right figure: rebar at the corner)

CONCLUSIONS

As the degree of pitting corrosion increases, the pressure require to cause cover cracking decreases greatly. The cracking pressures for non-uniform corrosion $\alpha = 4$ and $\alpha = 8$ are about 0.5 and 0.4 times of that of uniform corrosion (case $\alpha = 1$), respectively. As the cover to rebar diameter is increased, the pressure to cause cracking of the concrete cover increases with a linear relationship. As expected, the pressure required to cause cracking of the concrete cover increases as the concrete compressive strength increases. Good correlation between the models predicated cracking pressure and that obtained in the experiment is observed.

REFERENCES

WILLIAMSON, S. J., and CLARK, L. A.. "Pressure required to cause cover cracking of concrete due to reinforcement corrosion". *Magazine of Concrete Research*, 52 (6), 2000, 455-467.

LI, C. Q., W. LAWANWISUT, J. J. ZHENG, and W. KIJAWATWIRAWET. "Crack Width Due to corroded Bar in Reinforced Concrete Structures". *International Journal of Materials & Structural Reliability*, 3 (2), 2005, 87-94.

MACKERLE, J. "Finite-element modelling of non-destructive material evaluation". *Modelling Simulation Material Science Engineering*, 7, 1999, 107-145.

BIGGS, M., F. BARTON, J. GOMEZ, P. MASSARELLI, and W. MCKEEL. "Finite Element Modeling and Analysis of Reinforced-Concrete Bridge Decks". Virginia: University of Virginia. 2000

PARK, R., and T. PAULAY. *Reinforced Concrete Structures*, John Wiley & Sons, 1975.

WARNER, R., B. RANGAN, A. HALL, and K. FAULKES. *Concrete Structures*, Longman, 1998.

ARSLAN, G. "Sensitivity study of the Drucker-Prager modeling parameters in the prediction of the nonlinear response of reinforced concrete structures". *Materials & Design*, 28 (10), 2007, 2596-2603.

GONZALEZ, J. A., C. ANDRADE, C. ALONSO, and S. FELIU. "Comparison of Rates of General Corrosion and Maximum Pitting Penetration on Concrete Embedded Steel Reinforcement". *Cement and Concrete Research*, 25 (2), 1995, 257-264.

JANG, B. S., and B. H. OH. "Effects of non-uniform corrosion on the cracking and service life of reinforced concrete structures". *Cement and Concrete Research*, 40, 2010, 1441–1450.

Strand7. 2011. *Strand7 nonlinear static solver*. http://www.strand7.com/html/nonlinearstatic.htm